J. Appl. Cryst. (1997). **30**, 664–669

Isothermal Structural Evolution of SnO_2 Monolithic Porous Xerogels

G. E. S. BRITO,[a,b] S. H. PULCINELLI,[a] C. V. SANTILLI[a] AND A. F. CRAIEVICH[c]

[a] *Institute of Chemistry-UNESP, Araraquara, SP, Brazil,* [b] *LURE, Université Paris-Sud, Orsay, France, and* [c] *National Synchrotron Light Laboratory-CNPq, Campinas, SP, and Institute of Physics-USP, São Paulo, SP, Brazil. E-mail: santilli@iq.unesp.br*

(*Received 23 July 1996; accepted 7 February 1997*)

Abstract

Monolithic samples of SnO_2 xerogel were produced by careful control of the gelation and drying steps of material preparation. In these samples, small and nanoporous aggregates stick together, yielding a monolithic (nonpowdered) material. The material was analyzed by *in situ* small-angle X-ray scattering (SAXS) during isothermal treatment at temperatures ranging from 473 to 773 K. At 473 K, the SAXS intensity does not change significantly with time. All experimental scattering intensity functions for $T > 473$ K are composed of two wide peaks, which evolve with increasing time. Each of them was associated with one of the modes of a bimodal distribution of pore sizes corresponding to a fine (intra-aggregate) and a coarse (inter-aggregate) porosity. The SAXS intensities of the maxima of both peaks increase with increasing treatment time, while the position of their maxima, associated with an average correlation distance, decreases. The time dependences of the SAXS intensity corresponding to both families of pores qualitatively agree with those expected for a two-phase separating system exhibiting dynamic scaling properties. The time evolutions of the several moments of the structure function of samples heat treated at 773 K exhibit a good quantitative agreement with the theory of dynamic scaling for systems evolving by a coagulation mechanism. The kinetic parameters are the same for both peaks, indicating that the same mechanism is responsible for the structural evolution of both families of pores.

1. Introduction

It is known that nucleation and separation of one crystalline phase occur concomitantly with morphological and structural modifications during the heating of porous xerogels of sol–gel-derived glass ceramics (Brinker & Scherer, 1990). This makes the understanding of the properties of these materials difficult without experimental studies of their structural evolution. When the relevant structural features are heterogeneities, whose size ranges from about 10 up to 1000 Å, the small-angle X-ray scattering (SAXS) technique has proved to be useful for their characterization. In particular, *in situ* SAXS has been successively applied to the study of the dynamic aspects of phase separation (Craievich, Sanchez & Williams, 1986) and the densification of porous xerogels (Lours, Zarzycki, Craievich & Aegerter, 1990).

In previous studies of SnO_2 compacted sol–gel powders (Craievich, Santilli & Pulcinelli, 1995; Santilli, Pulcinelli & Craievich, 1995), a fraction of the total SAXS intensity was associated with the fine porosity existing inside the aggregates constituted of small particles, and the other fraction, at very small q values, with inter-aggregate pores. Under isothermal heat treatment between 673 and 873 K, no significant overall densification of the samples occurred and the growth of the fine porosity could be described by a statistical theory for structural evolutions exhibiting dynamic scaling properties (Marro, Lebowitz & Kalos, 1979). The main conclusion was that the theory predicting dynamic scaling properties of the structure function, first derived from basic statistical considerations for phase separation in binary solid solutions, has a wider domain of applicability. In the previous study of the compacted powder, the analysis only concerned the time evolution of the fine porosity, the inter-aggregate pores being too large to be characterized by SAXS methods.

In this paper, we report the structural evolution of monolithic SnO_2 thin plates containing intra- and inter-aggregate pores, both being small enough to be characterized by SAXS. *In situ* SAXS measurements were carried out during isothermal treatment at several temperatures, from 473 up to 773 K, with the aim of obtaining additional information on the structural evolution of SnO_2 porous xerogels.

2. Basic theory

Dynamic scaling properties were established for the phase-separation process in materials in which the fraction of the phases are time constant. In these materials, the growth process is invariant under a rescaling of distance and time t. As a consequence, the structural evolution of a system under these conditions can be

described by a single characteristic length $L(t)$ and the structure function $S(q, t)$, or the SAXS intensity $I(q, t)$, can be scaled according to (Furukawa, 1988)

$$I(q, t) = S(q, t) = L(t)^3 F[q, L(t), t] \qquad (1)$$

in which q is the modulus of the scattering vector. Different parameters have been used for $L(t)$, such as the gyration radius obtained from Guinier plots; or $L_m(t) = q_m^{-1}(t)$, q_m being the value corresponding to the maximum in the SAXS curve; or $L_1(t) = q_1^{-1}(t)$, q_1 being the first normalized moment of $I(q)$ defined by

$$q_1 = \int_0^\infty qI(q)\,\mathrm{d}q / \int_0^\infty I(q)\,\mathrm{d}q. \qquad (2)$$

Relevant parameters associated with the predictions of the dynamic scaling theory are the exponents associated with the time evolution of $q_m(t)$ and the maximum of the X-ray scattering intensity, $I_m(t)$, of the structure function

$$q_m(t) \propto t^{-\alpha} \qquad (3)$$

and

$$I_m(t) \propto t^{\alpha'}. \qquad (4)$$

The values of the kinetic exponents depend on the growth mechanism and the relationship $\alpha' = 3\alpha$ is often used for testing the scaling hypothesis (Furukawa, 1988).

The relationships between the moments

$$S_n(t) = \int_0^\infty q_n I(q, t)\,\mathrm{d}q \qquad (n = 0, 1, 2) \qquad (5)$$

and the first normalized moment q_1 are also used to verify the dynamic scaling property of the structure function. The scaling theory predicts that

$$S_n(t) = K_n[q_1(t)]^{n-2} \qquad (6)$$

K_n being equal to

$$K_n = \int_0^\infty x^n F(x)\mathrm{d}x, \qquad \text{with } x = q/q_1. \qquad (7)$$

Equation (6) implies that $S_2(t)$ is a time constant. This means that one of the conditions for the validity of the dynamic scaling hypothesis in two-phase systems is that the volume fractions of the phases do not vary with time (Glatter & Kratky, 1982).

3. Sample preparation

The samples were prepared from SnO_2 hydrosols synthesized by the sol–gel process described in an earlier paper (Hiratsuka, Santilli, Silva & Pulcinelli, 1992). The difference in preparation comes from gelation and drying, which were controlled, with the aim of producing thin plates with a thickness adequate for SAXS experiments. The gel plates were formed by pouring the aqueous colloidal suspensions onto a Teflon beaker containing a mixture of liquid paraffin and chloroform, which were chosen for their low reactivity and high density. As the suspension was poured, it spread over the bath remaining on the surface, permitting a large area of evaporation. During evaporation at room temperature, a flexible gel layer was first formed; this sheet was quickly dried, leading to a fragile sample. The dissolution of the paraffin film (remaining between the sample and the beaker) by washing with hexane permits the peeling of the sheet. The dried plates were typically 0.2 mm thick. This process of thin plate preparation was adapted from a method described by Klein (1988).

4. SAXS measurements

The SAXS experiments were carried out at the D24 workstation at the synchrotron radiation laboratory LURE, Orsay, France. In this workstation, the X-ray beam is horizontally focused and monochromatized by a bent silicon crystal ($\lambda = 1.49$ Å). Two sets of slits define a pinhole-like beam. The samples were held at constant temperature using a chamber stable within 1 K during the SAXS measurements at 473, 573, 673 and 773 K. SAXS spectra were recorded a few minutes after placing the gel plates into the high-temperature chamber.

The scattered intensity functions, $I(q)$, were determined as functions of the modulus of the scattering vector $\mathbf{q}$, using a vertical position-sensitive X-ray detector coupled to a standard multichannel analyzer. Parasitic air and slit scattering were subtracted from the total intensity. An ionization chamber, placed downstream from the sample, was used to monitor the intensity decay of the transmitted beam and to determine the sample attenuation. The natural decay in intensity of the incident beam was also monitored by recording the electronic current in the synchrotron source.

Because of the small size of the incident beam cross-section at the detection plane, no mathematical desmearing of the experimental data was necessary. Each spectrum corresponds to a data collection time interval of 300 s.

5. Results and discussion

Fig. 1(*a*) shows the SAXS intensities $I(q)$, or structure functions $S(q)$, measured during isothermal heating at 473, 573, 673 and 773 K. At 473 K, the SAXS intensity is almost time invariant and exhibits a sharp decrease with increasing q. At 573 K, a clear wide peak at small-angle develops and a shoulder at a higher q range is observed. The relative intensity of this shoulder is higher in samples heat treated at 673 K, giving rise in this case to two well defined peaks in the spectra. The relative

positions of both peaks indicate that the high-q peak is not the second-order scattering of the low-q one.

The position of the peak at high q range is comparable to that which was associated with a nanoporous structure in a previously studied compacted powdered xerogel (Craievich, Santilli & Pulcinelli, 1995; Santilli, Pulcinelli & Craievich, 1995). The peak at a lower q range was not observed in compacted powdered samples; instead a sharp increase in intensity for decreasing q was observed. This was attributed to the effect of a coarse

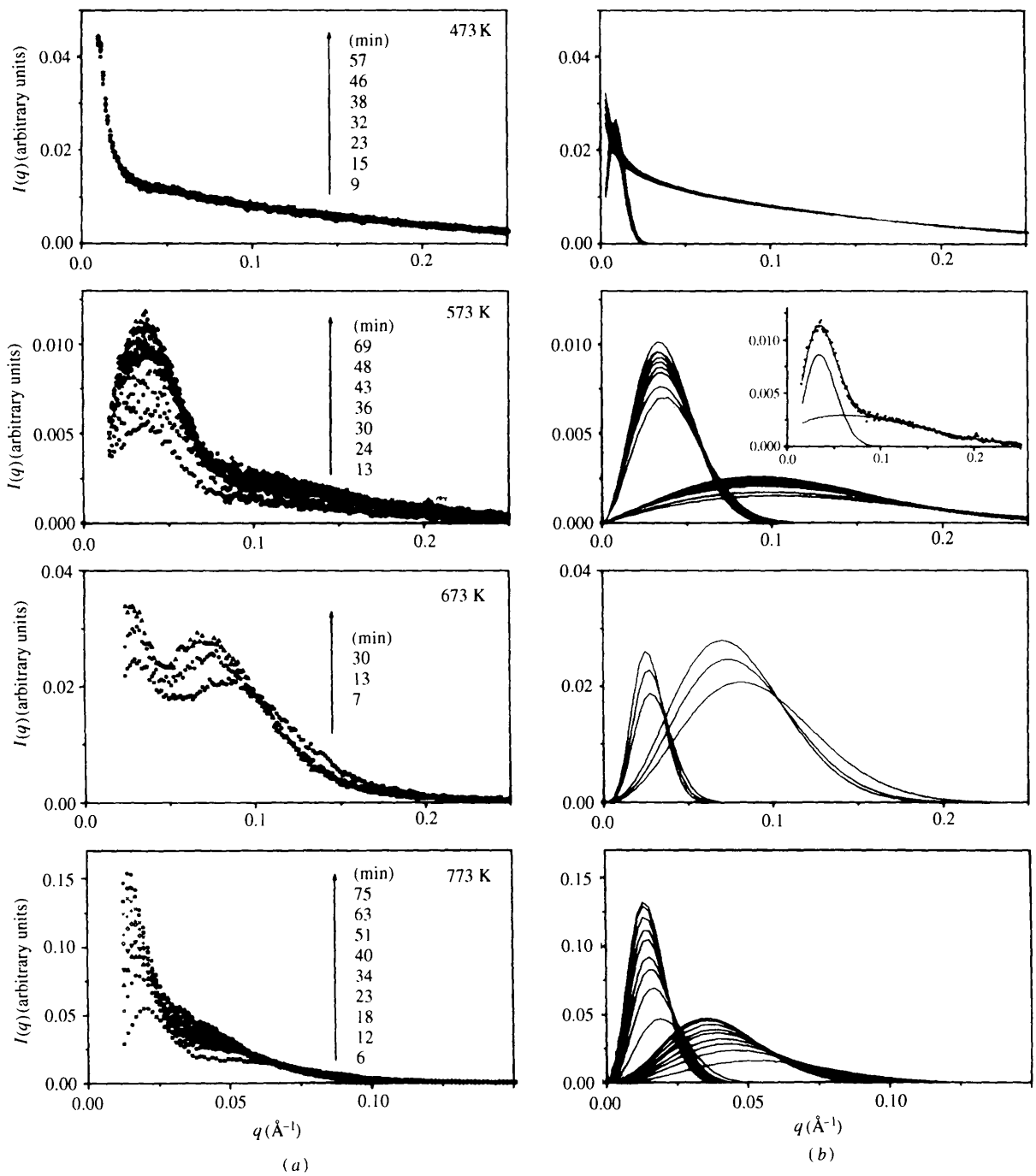

Fig. 1. Time evolution of the SAXS intensities as functions of the modulus of the scattering vector, measured at the indicated temperatures: (*a*) experimental curves; (*b*) individual peaks determined by fitting procedure. The insert in (*b*) at 573 K displays the peaks fitting at small and high q ranges, the total fitted curve and the experimental points.

porosity associated with the imperfect packing of the gel aggregates.

Taking into account the previous SAXS results and the conclusions from independent N_2 adsorption isothermal measurements (Brito, Pulcinelli & Santilli, 1994), the two-peak feature of the SAXS intensities shown in Fig. 1(*a*) was attributed to two porosity levels: (i) a fine nanoporosity inside the gel particle network (intra-aggregate porosity) associated with the peak at high q; and (ii) a mesoporosity between the gel particles (inter-aggregate porosity) associated with the small-q peak. This assumption also applies to the SAXS intensity corresponding to $T = 473$ K; at this temperature, the mesoporosity being coarser, the low-q peak is not apparent in the studied q domain.

We tried to establish if the evolution of SAXS intensity corresponding to each level of porosity, in samples treated at 573, 673 and 773 K, separately exhibits dynamic scaling properties. This analysis is only possible if the position and the intensity of the peak maxima are well defined, which is not the case for high-q peaks corresponding to samples treated at 573 and 773 K, as can be seen in Fig. 1(*a*). In order to solve this problem, the experimental SAXS intensities of Fig. 1(*a*) were approximated by a superposition of empirical two-peaked functions

$$I(q) = I_1(q) + I_2(q) = \sum_{i=1}^{2} a_i q^{b_i} \exp(-q^2 R_i^2/5) \qquad (8)$$

where the parameters a_i, b_i and R_i were determined by a nonlinear least-squares fitting procedure leading to an agreement factor

$$\rho = \frac{\sum_i [I_{\text{exp}}(q) - I_{\text{theor}}(q)]^2}{\sum_i [I_{\text{exp}}(q)]^2}$$

smaller than 10^{-7}.

The simple additivity of both contributions proposed by (8) assumes that the inter- and intra-aggregate porosity scatter independently. The time evolutions of the curves obtained by the fittings, $I_1(q)$ and $I_2(q)$, are shown for each temperature in Fig. 1(*b*). It should be pointed out that at 473 K the experimental SAXS intensity can also be approximated by (8). At this temperature, the correlation length L_m related to each peak maximum $[L_m(t) = 1/q_m(t)]$, is much larger than that observed at higher temperatures. This indicates that during heating from 473 to 573 K, an important structural rearrangement occurs, leading to the densification of the network packing inside the aggregates and between the aggregates. This interpretation agrees with the shrinkage effect associated with the dehydration reaction observed in this temperature range (Brito, Briois, Pulcinelli & Santilli, 1997).

During the isothermal treatment at 573 K, the positions of the maxima, $q_m(t)$, of both peaks decrease slightly, while the corresponding intensity, $I_m(t)$, increases. This behaviour is qualitatively similar to that observed in the first stage of domain formation with fixed size but increasing concentration difference (Kostorz, 1991). This implies that the morphology of the porosity in the gels held at 573 K does not change significantly, the intensity increase being related to the emptying of the pores due to the evaporation of the remaining structural water and OH groups.

The significant diminution of $q_m(t)$ and the increase in the intensity $I_m(t)$ observed for both peaks during isothermal treatment at 673 and 773 K indicate the existence of a structural coarsening of both types of porosity. Qualitatively, this is the behaviour which is expected from evolving two-electronic density systems having a constant contrast in electronic density and a constant volume fraction of both phases, and exhibiting the dynamic scaling properties described in §2.

The time evolution of the scattering vector $q_m(t)$ and the intensity $I_m(t)$ corresponding to the maximum of the fitted scattering curves from samples treated at 573, 673 and 773 K are presented in Fig. 2 in double logarithmic scale. This agrees with the power law dependence predicted by equations (3) and (4). However, the values of the exponent α are dependent both upon the temperature and upon the type of porosity.

The plots in Fig. 2 for samples treated at 673 K indicate that the exponents α are equal to 0.08 and 0.12 for the coarse and fine porosity, respectively. The exponents α' are both equal to 0.26. The relation

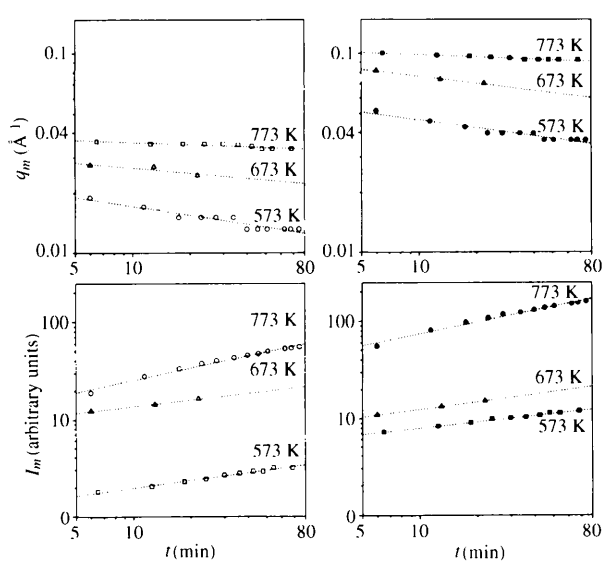

Fig. 2. Time evolution of the scattering vector $q_m(t)$ and SAXS intensity $I_m(t)$ corresponding to the maximum of the scattering curves of Fig. 1(*b*) for samples treated at the indicated temperatures. The curves correspond to the low-q peak profile (left) and the high-q profile (right).

$\alpha' = 3\alpha$, which is expected for systems with dynamic scaling properties, approximately holds only for the time evolution of the fine porosity. On the other hand, the integral $S_2(t)$ is not time constant, implying that the volume fractions vary with time and consequently that the theory of dynamic scaling does not apply to the structural evolution at 673 K.

The time evolutions of $q_m(t)$ of both peaks at 773 K (Fig. 2) exhibit nearly the same exponent ($\alpha = 0.14$). The difference in the values of the α exponent at 673 and 773 K indicates that the mechanism for porosity growth is temperature dependent. The value of 0.14 observed for the samples treated at 773 K is close to that theoretically predicted by Furukawa (1988) for solid cluster coagulation controlled by the surface mobility ($\alpha = 0.16$). On the other hand, the exponent $\alpha = 0.41$ is close to 3α as expected from the theory for dynamic scaling.

The calculations of the different moments of the SAXS spectra, $S_n(t)$, from samples treated at 773 K were carried out by integration of the $I_1(q)$ and $I_2(q)$ functions obtained from the fitting of the experimental $I(q)$ functions (Fig. 1*b*). The several moments $S_n(t)$ and the second normalized moment $q_2(t)$ are plotted in Fig. 3, in double logarithmic scale, as functions of $q_1(t)$. The linear behaviours predicted by (6) are, in general, obeyed. In particular, the time constancy of the second moment $S_2(t)$ demonstrates that the volume fraction occupied by the fine and the coarse porosity remains constant during the isothermal treatment, *i.e.* the migration of intra-pores to inter-aggregate pores and from these to the external surface does not occur.

The scaling property of the structure function is verified, as shown in Fig. 4. All the scattering intensities, corresponding to the different heat treatment times at 773 K and to both families of pores, collapse in a single scaled curve, demonstrating the scaling property of the structure function. The scaled function, being equivalent for both the low-q and high-q peak profiles, indicates that the mechanism for structural evolution is the same for both the fine intra-aggregate and the coarse inter-aggregate porosities.

Fig. 5 shows a schematic model for the structural evolution of SnO_2 xerogels based on the presented experimental SAXS results and others associated with previous independent measurements of transmission electron microscopy (TEM) (Pulcinelli, Santilli, Jolivet & Tronc, 1994) and N_2 adsorption analyses (Brito, Pulcinelli & Santilli, 1994). The observation of dried gels by means of TEM showed that the structure of the aggregates is a network of chains of small colloidal particles, ideally schematized in Fig. 5. The packing of the colloidal particles inside the aggregates and of the aggregates themselves is not compact and, as a consequence, a fine and a coarse porosity are formed, resulting in a bimodal pore size distribution (Brito, Pulcinelli & Santilli, 1994).

The large correlation lengths observed for samples treated at 473 K (Fig. 5*a*) are due to the presence of water and/or OH molecules on the surface of the primary particles (Brito, Briois, Pulcinelli & Santilli,

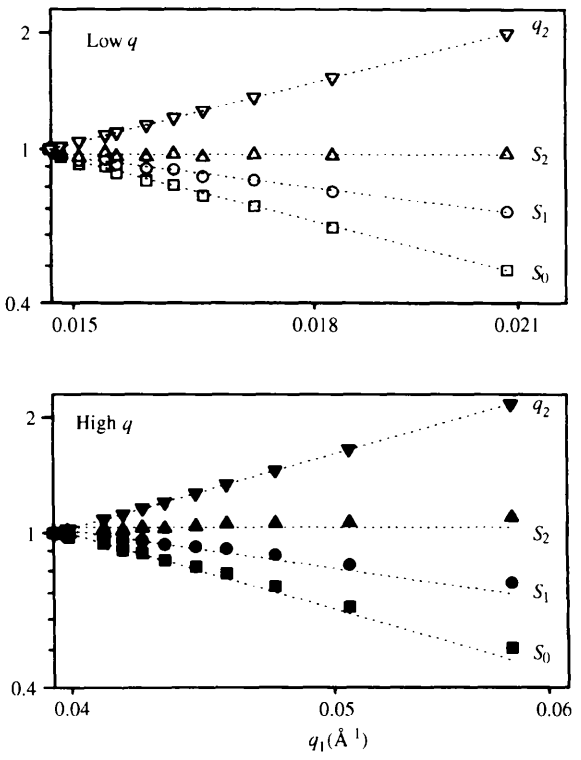

Fig. 3. Log–log plots of the normalized moments $S_0(t)/S_0(t_f)$, $S_1(t)/S_1(t_f)$, $S_2(t)/S_2(t_f)$ and $q_2(t)/q_2(t_f)$, as functions of $q_1(t)$, where t_f stands for the longest time of heating. The straight lines have the slopes predicted by the theory (-2, -1, 0 and 2, respectively).

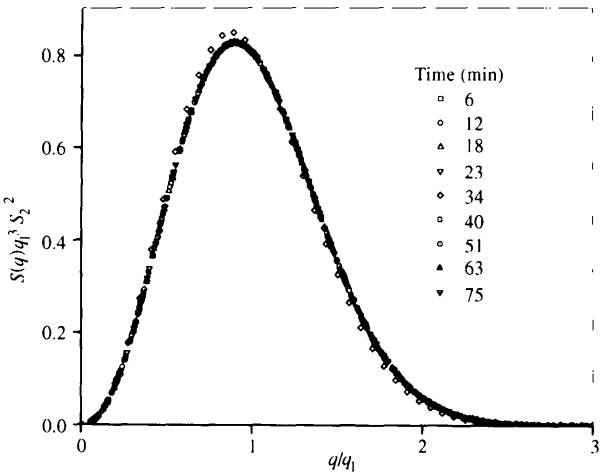

Fig. 4. The scaled structure function for samples treated at 773 K. Points corresponding to the low- and high-q peak profiles are plotted in black and white symbols, respectively.

1997). The dehydration reaction, which takes place during heating between 473 and 573 K, leads to the diminution of the distance between the colloidal particles, reducing the size of the fine pores. As a consequence, the chains shrink, eventually producing the breaking of chain junctions, which favours the structure network rearrangement and the body shrinkage observed by dilatometry (Brito, Brios, Pulcinelli & Santilli, 1997), which is represented by the decrease in the size of the rectangle from Fig. 5(*a*) to 5(*b*). This leads to the formation of nonperfectly packed nanoporous aggregates. This is a fast process expected to be driven by capillary strains from dehydroxylation of weakly linked molecules (hydrogen bonds). Both types of porosities exhibit a coarsening when treated isothermically at 573, 673 and 773 K.

6. Conclusion

This SAXS study, together with previous results of investigations using TEM and N_2 adsorption analyses, allowed us to establish the basic characteristics of the structural transformations of SnO_2 xerogels heated up to temperatures ranging from 473 to 773 K and held at them for different time intervals.

When monolithic xerogels are heated from 473 to 573 K, a strong decrease in pore correlation length occurs as a consequence of a shrinkage of the gel particle network. The SAXS intensity or structure function corresponding to the porous xerogel heated to 573 K exhibits two well defined characteristic peaks which we attributed to the existence of a bimodal (intra- and inter-aggregate) porosity.

The SAXS intensity functions corresponding to xerogels treated isothermally at 573 and 673 K for increasing time intervals are also consistent with a model of a bimodal porosity. Each type of porosity coarsens independently, similar to classical phase-separating systems exhibiting dynamic scaling properties for the structure function.

During isothermal treatment of the xerogel at 773 K, the structure functions associated with both porosities evolve in good quantitative agreement with the statistical theory which predicts dynamic scaling properties. The evolutions of the structure functions corresponding to the coarse and fine porosities have the same kinetic exponent, corresponding to a coarsening process controlled by coagulation. The scaled structure functions associated with the intra- and inter-aggregate porosities are equivalent, indicating that both types of porosity evolve independently but under similar structural conditions.

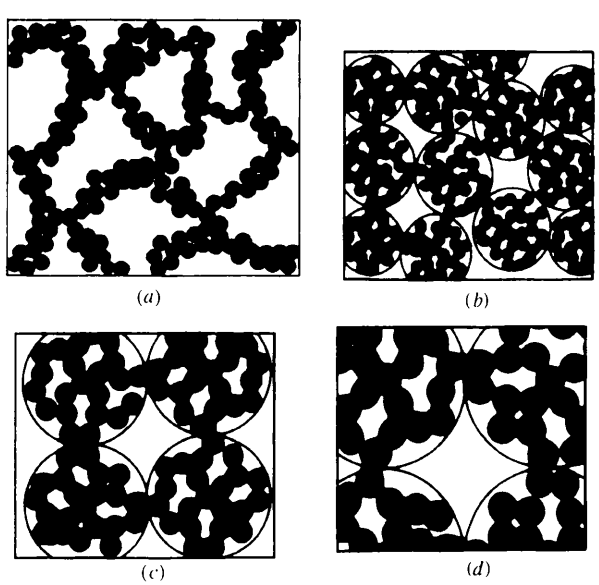

Fig. 5. Schematic model proposed for the structural evolution of the two pore levels of the SnO_2 xerogel during heating at (*a*) 473 K, (*b*) 573 K, (*c*) 673 K and (*d*) 773 K.

The authors thank V. Briois for her assistance. This work has been supported by CNPq, CAPES/COFECUB and FAPESP (Brazil).

References

Brinker, C. J. & Scherer, G. W. (1990). *Sol–Gel Science: The Physics and Chemistry of Sol–Gel Processing*, pp. 547–599. New York: Academic Press.

Brito, G. E. S., Briois, V., Pulcinelli, S. H. & Santilli, C. V. (1997). *J. Sol–Gel Sci. Technol.* **8**, 269–274.

Brito, G. E. S., Pulcinelli, S. H. & Santilli, C. V. (1994). *J. Sol–Gel Sci. Technol.* **2**, 575–579.

Craievich, A. F., Sanchez, J. M. & Williams, C. E. (1986). *Phys. Rev. B***34**, 2762–2769.

Craievich, A. F., Santilli, C. V. & Pulcinelli, S. H. (1995). *Nucl. Instrum. Methods Phys. Res. B***97**, 78–81.

Furukawa, H. J. (1988). *J. Appl. Cryst.* **21**, 805–810.

Glatter, O. & Kratky, O. (1982). *Small X-Rays Scattering*, pp. 199–230. London: Academic Press.

Hiratsuka, R. S., Santilli, C. V., Silva, D. V. & Pulcinelli, S. H. (1992). *J. Non Cryst. Solids*, **147**, **148**, 67–73.

Klein, L. C. (1988). *Sol–Gel Technology for Thin Films, Fibers, Preforms, Electronics and Speciality Shapes*, edited by L. C. Klein, pp. 382–398. New Jersey: Noyes.

Kostorz, G. (1991). *J. Appl. Cryst.* **24**, 444–456.

Lours, T., Zarzycki, J., Craievich, A. F. & Aegerter, M. A. (1990). *J. Non Cryst. Solids*, **121**, 216–220.

Marro, J., Lebowitz, J. L. & Kalos, M. H. (1979). *Phys. Rev. Lett.* **43**, 282–285.

Pulcinelli, S. H., Santilli, C. V., Jolivet, J. P. & Tronc, E. (1994). *J. Non Cryst. Solids*, **170**, 21–26.

Santilli, C. V., Pulcinelli, S. H. & Craievich, A. F. (1995). *Phys. Rev. B***51**, 8801–8809.